



**HAL**  
open science

## The role of platelets in blood coagulation during thrombus formation in flow

Alen Tosenberger, Fazly Ataulakhanov, Nikolai Bessonov, Mikhail A. Panteleev, Alexey Tokarev, Vitaly Volpert

► **To cite this version:**

Alen Tosenberger, Fazly Ataulakhanov, Nikolai Bessonov, Mikhail A. Panteleev, Alexey Tokarev, et al.. The role of platelets in blood coagulation during thrombus formation in flow. 2012. hal-00729046v1

**HAL Id: hal-00729046**

**<https://hal.science/hal-00729046v1>**

Preprint submitted on 7 Sep 2012 (v1), last revised 13 Sep 2012 (v2)

**HAL** is a multi-disciplinary open access archive for the deposit and dissemination of scientific research documents, whether they are published or not. The documents may come from teaching and research institutions in France or abroad, or from public or private research centers.

L'archive ouverte pluridisciplinaire **HAL**, est destinée au dépôt et à la diffusion de documents scientifiques de niveau recherche, publiés ou non, émanant des établissements d'enseignement et de recherche français ou étrangers, des laboratoires publics ou privés.

# The role of platelets in blood coagulation during thrombus formation in flow

A. Tosenberger<sup>1,2</sup>, F. Ataullakhanov<sup>3,4,5,6</sup>, N. Bessonov<sup>7</sup>, M. Panteleev<sup>3,4,5,6</sup>  
A. Tokarev<sup>3,4</sup>, V. Volpert<sup>1,2,8</sup>

<sup>1</sup> Institut Camille Jordan, UMR 5208 CNRS, University Lyon 1  
69622 Villeurbanne, France

<sup>2</sup> INRIA Team Dracula, INRIA Antenne Lyon la Doua 69603 Villeurbanne, France

<sup>3</sup> National Research Center for Haematology  
Ministry of Health and Social Development of Russian Federation  
Russia, 125167, Moscow, Novii Zykovskii pr., 4a

<sup>4</sup> Federal Research and Clinical Centre of Paediatric Haematology, Oncology and Immunology  
Ministry of Health and Social Development of Russian Federation  
Russia, 117198, Moscow, Samori Marshela str., 1

<sup>5</sup> Faculty of Physics, M. V. Lomonosov Moscow State University  
Russia, 119991, Moscow, GSP-1, 1-2 Leninskiye Gory

<sup>6</sup> Center for Theoretical Problems of Physicochemical Pharmacology  
Russian Academy of Sciences, Russia, 119991, Moscow, Kosygina str., 4

<sup>7</sup> Institute of Mechanical Engineering Problems, 199178 Saint Petersburg, Russia

<sup>8</sup> European Institute of Systems Biology and Medicine, 69007 Lyon, France

**Abstract.** Hemostatic plug covering the injury site (or a thrombus in the pathological case) is formed due to the complex interaction of aggregating platelets with biochemical reactions in plasma that participate in blood coagulation. The mechanisms that control clot growth and which lead to growth arrest are not yet completely understood. We model them with numerical simulations based on a hybrid DPD-PDE model. Dissipative particle dynamics (DPD) is used to model plasma flow with platelets while fibrin concentration is described by a simplified reaction-diffusion-convection equation.

The model takes into account consecutive stages of clot growth. First, a platelet is weakly connected to the clot and after some time this connection becomes stronger due to other surface receptors involved in platelet adhesion. At the same time, the fibrin network is formed inside the clot. This becomes possible because flow does not penetrate the clot and cannot wash out the reactants participating in blood coagulation. Platelets covered by the fibrin network cannot attach new platelets. Modelling shows that the growth of a hemostatic

plug can stop as a result of its exterior part being removed by the flow thus exposing its non-adhesive core to the flow.

## 1 Introduction

Hemostasis is a protective physiological mechanism that functions to stop bleeding upon vascular injury by sealing the wound with aggregates of specialized blood cells, platelets, and with gelatinous fibrin clots. Disorders of this system are the leading immediate cause of mortality and morbidity in the modern society. The most prominent of them is thrombosis, the intravascular formation of clots that obstruct blood flow in the vessels. Life-threatening thrombus formation is an ubiquitous complication or even cause of numerous diseases and conditions such as atherosclerosis, trauma, stroke, infarction, cancer, sepsis, surgery and others. To provide only one example, 70% of sudden cardiac deaths are due to thrombosis [1]; and the sudden cardiac deaths annually kill approximately 400 000 people in the United States only [2]. Development of thrombosis diagnostics and antithrombotic therapy is hampered by the incredible complexity of the hemostatic system comprising thousands of biochemical reactions of coagulation and platelet signaling that occur in the presence of spatial heterogeneity, cell reorganization and blood flow. The most promising pathway to resolving this problem is systems biology – a novel multidisciplinary science aimed at quantitative analysis and understanding of complex biological systems with the help of high-throughput experimental methods and computational modelling approaches. During the last 20 years, the hemostasis system was a subject of intense interest in this field; reviews are available that describe these theoretical studies of blood coagulation [3, 4] and platelet-dependent hemostasis and thrombosis [4, 5, 6]. In recent years, computational modeling of coagulation has become a very widely used tool for investigation of the mechanisms of drug action, optimization of therapy, analysis of drug-drug interaction at early stages (e.g. see recent examples for direct factor Xa inhibitors, novel anti-TFPI aptamer and recombinant activated factor VIII [7, 8, 9]). However, numerous problems remain. There is currently no mathematical model that could adequately account for all innumerable aspects of thrombosis and hemostasis; even the best ones usually use very unreliable assumptions about platelets, biochemistry and hydrodynamics. The solution of these problems requires a close cooperation between specialists in the hemostasis field and those in computational mathematics. This paper provides a brief review of the field from a biological and medical point of view, followed by a computational analysis of the problem of thrombus formation using dissipative particle dynamics methods.

## 2 Platelets, flow, and blood coagulation

Hemostasis is a protective physiological mechanism that functions to stop hemorrhage upon vascular injury. The two principal components of hemostasis are: i) platelets, specialized cells that adhere to the damaged tissue and form a primary plug reducing blood loss (Figure 1A); ii) blood coagulation, a complex reaction network that turns fluid plasma into a solid fibrin gel to completely seal the wound (Figure 1B). Maintaining the delicate balance between the fluid and the solid states of blood is not simple, and a lion's share among the causes of mortality and morbidity in the modern society belongs to hemostatic disorders. The leading one is thrombosis, intravascular formation of platelet-fibrin clots that obstruct blood flow in the vessels. The major obstruction for prevention and treatment of thrombosis is insufficient knowledge of its regulation mechanisms. Platelet aggregation and blood coagulation are extremely complex processes. The attachment of platelets and their accumulation into a thrombus is regulated by mechanical interactions with erythrocytes and the vessel wall, by numerous chemical agents such as thrombin, or ADP, or prostaglandins, or collagen, as well as by an enormous network of intracellular signaling. Blood coagulation is only marginally simpler, including some fifty proteins that interact with each other and with blood or vascular cells in approximately two hundred reactions in the presence of flow and diffusion.

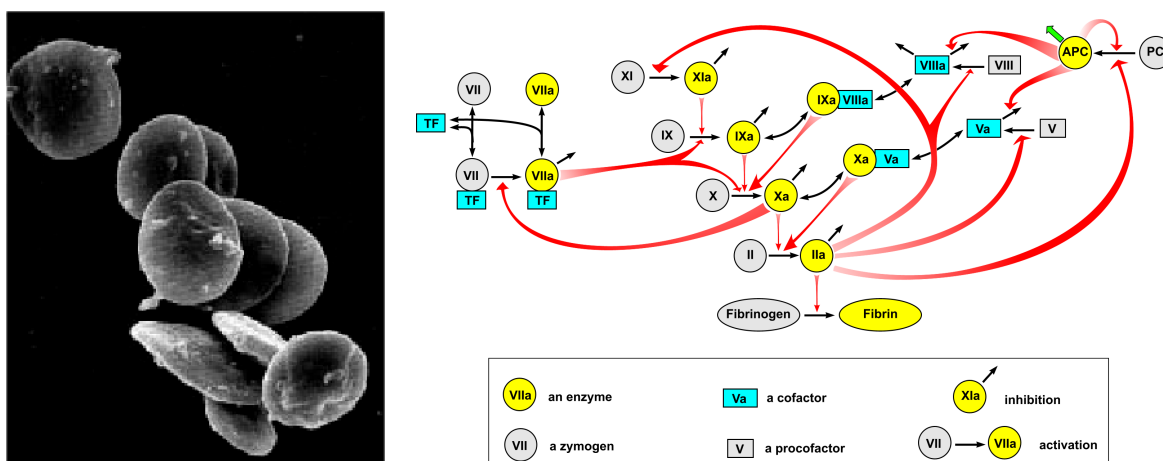


Figure 1: Two components of hemostasis. (A) Electron microphotograph of blood platelets [10]. Platelets are small discoid anucleate cells able to undergo activation in case of vascular damage to form hemostatic plugs or pathological thrombi. (B) Main reactions of blood coagulation [11], a reaction cascade that is initiated by tissue factor exposure at the site of damage and produces fibrin, which polymerizes to create a gelatinous clot.

Although extensive research during the last decades identified many key players in the hemostatic system, the regulation of hemostasis and thrombosis remains poorly understood. It is extremely difficult to relate a protein or a reaction in such a complex system to the functioning of the system as a whole. The most crucial unresolved problem is the very difference

between hemostasis and thrombosis. All existing anticoagulants cannot tell them apart and target indiscriminately (that is why it is impossible to prevent coronary artery thrombosis simply by putting all persons in high risk groups on anticoagulation therapy: the possibility of death from external bleeding or a cerebral hemorrhage would become too high). If we knew these mechanisms, it would be possible to target them specifically in order to inhibit intravascular thrombi and prevent blood vessel occlusion while leaving the hemostatic functions relatively intact. The most advanced and powerful pathway to decomposing complex systems in systems biology is developing a comprehensive mathematical model and then subjecting it to a sensitivity analysis in a sort of "middle-out" approach; an example of modular decomposition for the blood coagulation cascade can be found in [11]. The most important problem that is hampering the application of this solution is that thrombosis and hemostasis cannot be completely understood without combining all three essential elements: platelets, coagulation, and flow.

By forming aggregates, blood platelets build hemostatic plugs and thrombi. This process cannot proceed without flow, and is strongly dependent on platelet-erythrocyte interaction in the presence of flow [12]. Blood coagulation is important for platelet plug formation, because thrombin is one of the main activators of platelets ensuring thrombus/plug stability, and because the fibrin network solidifies the cell aggregate. In contrast, blood coagulation is strongly inhibited by flow. Active coagulation factors are removed from the site of injury to such a degree that no fibrin clot can be formed at a physiological arterial shear rate [13]. Therefore, thrombus formation in the presence of a rapid flow requires platelets that mechanically protect coagulation from the flow, provide binding sites for coagulation factors and secrete substances that participate in coagulation such as fibrinogen, factor V, XI, etc.

One of the most intriguing problems in the field of thrombosis is the problem of regulating the size of the thrombus. While the mechanisms of thrombus growth became well established during the last decade [14], it is not clear how and when a thrombus stops to grow in order to avoid a complete occlusion of the vessel. One thing that is firmly established is that an occlusion does not always occur: while the popular experimental model of ferric-chloride induced damage to the carotid artery usually ends with an occlusion [15], there is no occlusion in the laser-induced injury model of thrombosis in small arterioles [16]. Numerous hypothesis have been proposed to explain the mechanism of thrombus growth stopping (e.g. the role of thrombomodulin [17]). One of the most intriguing is the role of fibrin clot - platelet thrombus interaction: it suggests the formation of a fibrin cap on the surface of the thrombus that prevents further platelet accumulation [18]. However, the formation of fibrin on the surface of a thrombus is unlikely because of high shear rates that remove active coagulation factors [13]. In other words, the fibrin formation can occur only under the protection of platelets, therefore the formation of a fibrin cap cannot occur on the surface of the platelet thrombus. For that reason we expand this hypothesis by taking into account the disruption of the platelet thrombus. This disruption can destroy the unstable outer part of the thrombus and reveal the under-laying fibrin-cemented part, which can then function as the cap preventing

further adhesion. In the pursuit of a biologically correct mathematical model we begin by building a hybrid model which couples the DPD particle method with one convection-reaction-diffusion equation. The first method is used for the modelling of blood plasma flow and platelet interaction. The latter method is used to describe the concentration of blood factors, i.e. their production and dissipation in the flow. In this article two models are described. The first model is discrete, while the second model continues on the first one by adding the convection-reaction-diffusion equation.

### 3 Numerical simulations of clot growth

#### 3.1 DPD

We use the Dissipative Particle Dynamics (DPD) method in the form described in literature [20, 21, 22]. It is a mesoscale method, meaning that each DPD particle describes some small volume of a simulated medium rather than an individual molecule. The method is governed by three equations describing the conservative, dissipative and random force acting between each two particles:

$$\mathbf{F}_{ij}^C = F_{ij}^C(r_{ij})\hat{\mathbf{r}}_{ij}, \quad (1)$$

$$\mathbf{F}_{ij}^D = -\gamma\omega^D(r_{ij})(\mathbf{v}_{ij} \cdot \hat{\mathbf{r}}_{ij})\hat{\mathbf{r}}_{ij}, \quad (2)$$

$$\mathbf{F}_{ij}^R = \sigma\omega^R(r_{ij})\frac{\xi_{ij}}{\sqrt{dt}}\hat{\mathbf{r}}_{ij}, \quad (3)$$

where  $\mathbf{r}_i$  is the vector of position of the particle  $i$ ,  $\mathbf{r}_{ij} = \mathbf{r}_i - \mathbf{r}_j$ ,  $r_{ij} = |\mathbf{r}_{ij}|$ ,  $\hat{\mathbf{r}}_{ij} = \mathbf{r}_{ij}/r_{ij}$ , and  $\mathbf{v}_{ij} = \mathbf{v}_i - \mathbf{v}_j$  is the difference between velocities of two particles,  $\gamma$  and  $\sigma$  are coefficients which determine the strength of the dissipative and the random force respectively, while  $\omega^D$  and  $\omega^R$  are weight functions;  $\xi_{ij}$  is a normally distributed random variable with zero mean, unit variance, and  $\xi_{ij} = \xi_{ji}$ . The conservative force is given by the equality

$$F_{ij}^C(r_{ij}) = \begin{cases} a_{ij}(1 - r_{ij}/r_c) & \text{for } r_{ij} \leq r_c, \\ 0 & \text{for } r_{ij} > r_c, \end{cases} \quad (4)$$

where  $a_{ij}$  is the conservative force coefficient between particles  $i$  and  $j$ , and  $r_c$  is the cut-off radius.

The random and dissipative forces form a thermostat. If the following two relations are satisfied, the system will preserve its energy and maintain the equilibrium temperature:

$$\omega^D(r_{ij}) = [\omega^R(r_{ij})]^2, \quad \sigma^2 = 2\gamma k_B T, \quad (5)$$

where  $k_B$  is the Boltzmann constant and  $T$  is the temperature. The weight functions are determined by:

$$\omega^R(r_{ij}) = \begin{cases} (1 - r_{ij}/r_c)^k & \text{for } r_{ij} \leq r_c, \\ 0 & \text{for } r_{ij} > r_c, \end{cases} \quad (6)$$

where  $k = 1$  for the original DPD method, but it can be also varied in order to change the dynamic viscosity of the simulated fluid [20]. The motion of particles is determined by Newton's second law of motion:

$$d\mathbf{r}_i = \mathbf{v}_i dt, \quad d\mathbf{v}_i = \frac{dt}{m_i} \sum_{j \neq i} (\mathbf{F}_{ij}^C + \mathbf{F}_{ij}^D + \mathbf{F}_{ij}^R), \quad (7)$$

where  $m_i$  is the mass of the particle  $i$ .

Euler method or a modified version of the velocity-Verlet method [21, 23], which is more accurate, can be used to integrate the equations (7). In the former,

$$\mathbf{v}_i^{n+1} = \mathbf{v}_i^n + \frac{1}{m_i} \mathbf{F}_i(\mathbf{r}_i^n, \mathbf{v}_i^n) dt, \quad (8)$$

$$\mathbf{r}_i^{n+1} = \mathbf{r}_i^n + \mathbf{v}_i^{n+1} dt, \quad (9)$$

where indices  $n$  and  $n + 1$  denote time steps, and

$$\mathbf{F}_i = \sum_{j \neq i} (\mathbf{F}_{ij}^C + \mathbf{F}_{ij}^D + \mathbf{F}_{ij}^R). \quad (10)$$

The discretization in the second method is as follows:

$$\mathbf{r}_i^{n+1} = \mathbf{r}_i^n + \mathbf{v}_i^n dt + \frac{1}{2} \mathbf{a}_i^n dt^2, \quad (11)$$

$$\mathbf{v}_i^{n+\frac{1}{2}} = \mathbf{v}_i^n + \frac{1}{2} \mathbf{a}_i^n dt, \quad (12)$$

$$\mathbf{a}_i^{n+1} = \frac{1}{m_i} \mathbf{F}_i(\mathbf{r}_i^{n+1}, \mathbf{v}_i^{n+\frac{1}{2}}), \quad (13)$$

$$\mathbf{v}_i^{n+1} = \mathbf{v}_i^{n+\frac{1}{2}} + \frac{1}{2} \mathbf{a}_i^{n+1} dt, \quad (14)$$

where  $a_i^n$  denotes the acceleration of the particle  $i$  at the  $n^{\text{th}}$  time step. Both methods give close results.

The behaviour of DPD method, as well as its suitability for the problem of fluid simulation is well described in literature [20, 21, 22, 24, 25]. In [20, 24] DPD simulation results are compared with the results obtained by using continuous methods (Navier-Stokes and Stokes equations) for Couette, Poiseuille, square-cavity and triangular-cavity flow.

## 3.2 Platelet clot

### 3.2.1 Platelet aggregation

Platelets are modelled as soft spherical particles similar to the particles of fluid in DPD. The radius of all particles (fluid and platelets) and their mass are chosen to correspond to the radius and the mass of platelets. In our simulation the physical radius is set to  $1\mu\text{m}$  and the mass is chosen in such a way that particle density corresponds to the density of the blood plasma ( $\approx 10^3\text{kg/m}^3$ ). The interactions between all particles are then governed by DPD as described in the previous section with an additional adhesion force acting between platelets. By virtue of the mechanical properties of the clot [27, 28], the adhesion force is modelled as a pairwise force between two platelets expressed in the form of Hooke's law:

$$\mathbf{F}_{ij}^A = f^A(t_{ij}) \left(1 - \frac{r_{ij}}{d_C}\right) \hat{\mathbf{r}}_{ij}, \quad (15)$$

where  $f^A$  is the force strength coefficient and  $d_C$  is the force relaxation distance which is equal to two times the physical radius of the platelets. As platelet binding occurs due to their surface adhesion receptors, two platelets in a flow connect when they come in physical contact, i.e.  $r_{ij} \leq d_C$  (connection criterium). Platelets remain connected until their distance does not exceed a critical value  $d_D$  (disconnection criterium) which is greater than  $d_C$ . We set  $d_D$  equal to 1.5 times of the platelet diameter.

Platelet adhesion is a complex multi-step process which involves adhesion receptors of at least two different types and the process of platelet activation [19, 29, 30]. First, the platelet is captured from the flow through weak GPIIb/IIIa bonding, then it activates and forms stable adhesion through firm integrin bonding. The latter step cannot take place without the first one due to kinetic restrictions, and the first step is reversible and cannot result in stable adhesion. Since we do not explicitly introduce kinetics of receptor binding in the model, we need to take into account the time evolution of the adhesion force. Adhesion becomes stronger with time. For that reason the force strength coefficient  $f^A$  in equation (15) is modelled as a time dependant function:



$$f^A(t_{ij}) = \begin{cases} f_w^A & \text{if } t_{ij} < t_c, \\ f_s^A & \text{otherwise} \end{cases} \quad (16)$$

where  $f_w^A$  is the strength coefficient of the weaker connection,  $f_s^A$  is the strength coefficient of the stronger connection, and  $t_c$  is the time needed for the weak connection to transform into the stronger one. If a platelet is connected with the clot by at least one strong connection, it is considered to be a part of the clot core. We impose the condition that such platelets cannot establish any new connections and attach new platelets. At this stage of modelling, this condition mimics the role of fibrin network which covers platelets and prevents other platelets to adhere. In Section 3.4, 3.5 we will explicitly introduce fibrin in the model and will distinguish the platelets which have strong connection and which are non-adherent. In the case of physical contact between two platelets, one of which is non-adhesive, an additional repulsing force has to be introduced between them in order to prevent them from occupying the same space.

### 3.2.2 Clot growth

The values of parameters were chosen in such a way that they correspond to the vessel of  $50\mu m$  in diameter and  $150\mu m$  long. The density and the viscosity of the simulated medium were chosen to correspond to the density and viscosity of blood plasma [26] ( $\approx 1.24mPa\cdot s$ ). The average velocity of the flow is chosen to be  $24mm/s$ . To initiate clotting, at the beginning of the simulation, several stationary platelets are positioned next to the lower vessel wall.

Figure 2 shows results of Poiseuille flow simulated with DPD method and with the values of parameters indicated above. The density distribution is uniform and the distribution of velocity in the direction tangential to the vessel wall is parabolic. Velocity and density profiles were obtained by averaging particles' density and velocity through  $10^5$  time steps. As the clot grows and the vessel narrows, the velocity profile changes and shows an increase in velocity in the clot region (Figure 2 right).

The purpose of the discrete model version is to study the clot growth and its dependence on the platelet adhesion force as well as on the velocity of the flow, which can influence clot growth and disruption. The latter can occur due to the flow pressure on the clot.

The use of time dependant platelet adhesion force allows the creation of a clot core, in which the forces between platelets are stronger than the ones between the newly connected platelets in the outer part of the clot. The force ageing is modelled with a step function (equation (16)), which can be justified from the biological point of view - the transformation from weak reversible connections between platelets to strong irreversible ones happens quite quickly compared to the total time needed to complete the coagulation process. The key

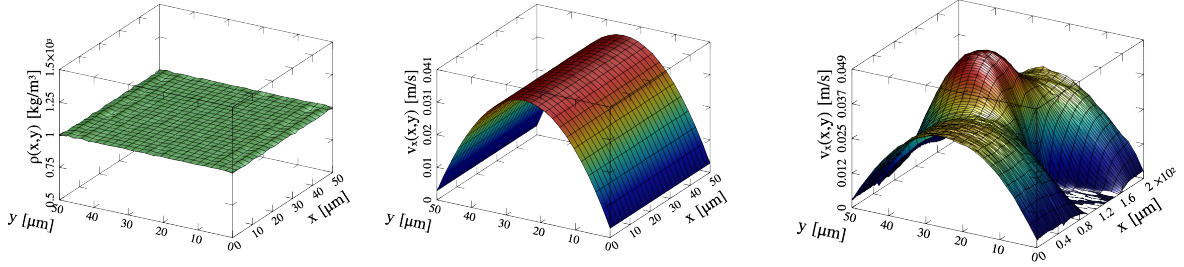


Figure 2: Poiseuille flow simulated with DPD: uniform density distribution (left) and parabolic velocity distribution (middle). The change in the velocity profile as the result of the clot formation (right).

moments of the simulation done with a step function model can be seen in Figure 3. The clot grows and at the same time the core of the clot forms. After the exterior part of the clot has been removed by the flow, the clot core stays attached to the blood vessel wall.

In Figure 4 two graphs are presented. The left graph presents the model behaviour without the condition that the platelets in the clot core become resistant to establishing of new connections. The graph shows how after some time the clot core forms, and that after the several following ruptures, due to the flow pressure on the clot, the clot core remains of approximatively the same size. In the case when the resistance condition is included in the model, after the formation of the clot core, and once it is revealed to the flow by ruptures of the weakly connected clot cap, the clot growth is stopped (Figure 4, right). Figure 5 shows formations of the clot core for two different adhesion force coefficients. In order to decrease the duration of simulations, the density of platelets in the blood flow is significantly increased and the time period  $t_c$  in the step function is decreased (equation (16)). Qualitatively, this has no influence on the results.

### 3.3 Platelet and fibrin clot

#### 3.3.1 Fibrin concentration

The formation of the fibrin net is responsible for the creation of the clot core and the clot growth arrest. Hence, the next step in modelling is to describe more precisely the biological mechanisms which regulate the process of blood coagulation. The proteins which control the process of coagulation are modelled by partial differential equations. This enables the description of their production, diffusion in the flow, and interaction with the blood flow velocity field via the convection term. Because of the complexity of the coagulation process, we begin by introducing just one reaction-diffusion-convection equation as the continuous

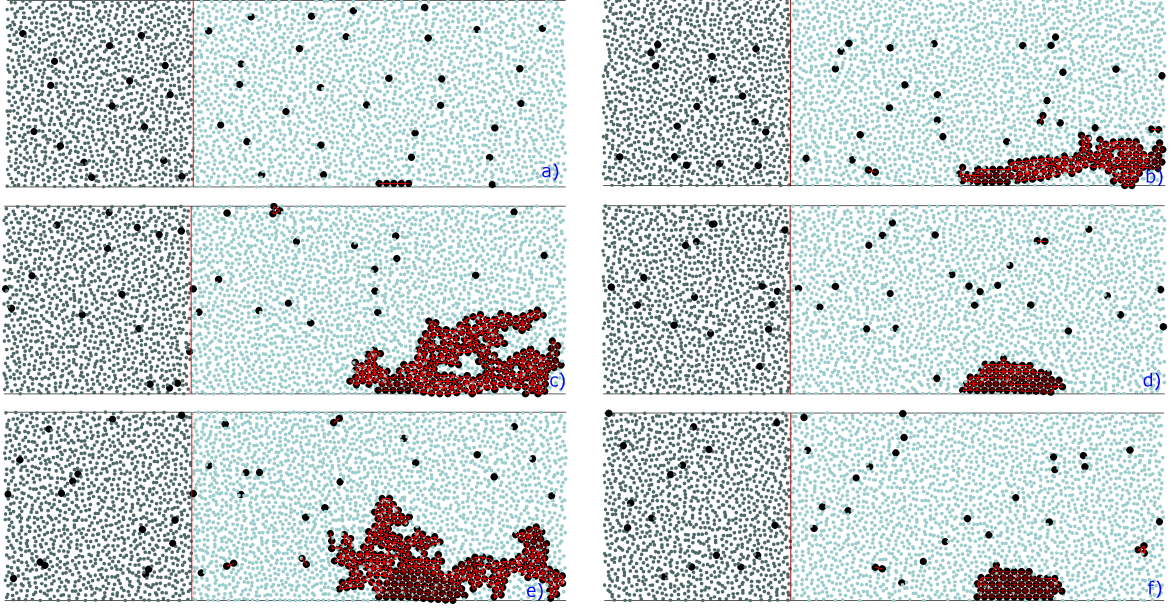


Figure 3: Snapshots of clot growth for step time dependant adhesion force (older connections are depicted with darker red colour): a) initial clot, b) and c) elongated clot with mainly weak connections, d) clot core with mainly strong connections after rupture, e) continued clot growth, f) fully formed clot core after rupture

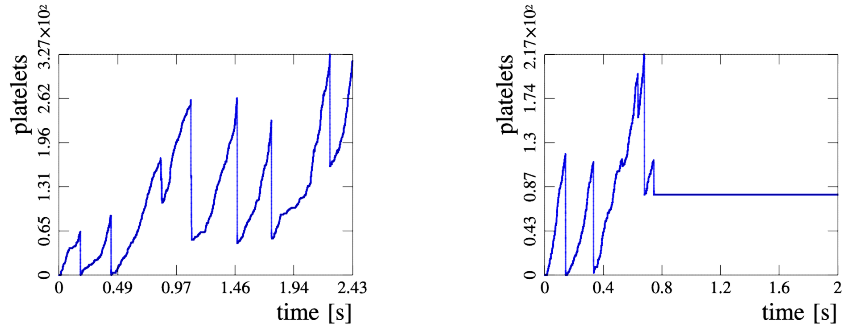


Figure 4: Clot growth and disruption for the discrete model - without (left) and with (right) the resistance condition.

part of the model. Here, the PDE describes a concentration of fibrin in the flow:

$$\frac{\partial u}{\partial t} = \alpha \Delta u - \nabla \cdot (\mathbf{v}u) + \beta u (1 - u), \quad (17)$$

where  $u$  is the fibrin concentration and  $v$  is the flow velocity. It is a model equation which does not correspond to detailed kinetics of blood coagulation but which allows us to capture all the main aspects of clot growth: the production and propagation of the concentration

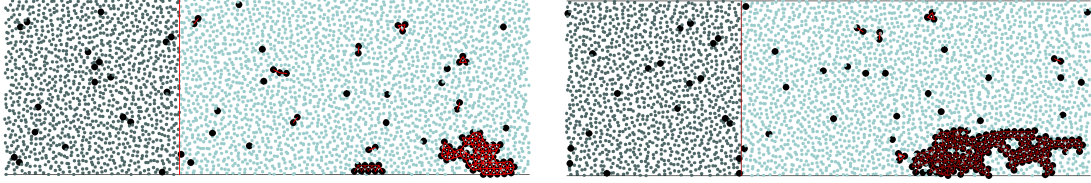


Figure 5: Discrete model: form of the clot core after the arrest of the clot growth for two different adhesion force parameters.

field and its interaction with the flow and with the clot.

To simulate the resistance of an already formed clot to the binding of free platelets from the flow, the critical concentration  $c_f$  is introduced. If the concentration is less than  $c_f$ , a platelet can bind with another platelet, if not, it will be resistant to adhesion. Accordingly, the platelet is considered to be a part of the clot core if it is in the clot and the fibrin concentration has been larger than  $c_f$  at the position of that platelet. As the clot grows, the plasma velocity in the region covered by the clot will be near zero compared to the average flow velocity in the whole domain, thus protecting the fibrin concentration from being driven away by the flow. This results in the gradual covering of the clot by a fibrin mesh (described by the PDE). Once the clot is completely covered by the fibrin mesh, it stops growing. Therefore, the use of fibrin concentration replaces the artificial resistance condition described in the discrete model.

Since DPD and the partial differential equation are solved with separate methods, an exchange period  $\tau$  is introduced as a parameter. At first the particle system is simulated for the  $\tau$  period of time. During that time the velocity profile is measured, and afterwards it is passed as a parameter to the partial differential equation. The PDE is then simulated for the  $\tau$  period, and the concentration profile is passed as a parameter to DPD, which finishes one  $\tau$ -cycle of the model (Figure 12).

### 3.3.2 Clot growth

As the clot grows it also protects the fibrin concentration from being taken by the flow. Several stages of the clot growth and the evolution of the fibrin concentration profile protected by the clot are shown in Figure 7 and Figure 8. The clot grows until it is completely covered by the fibrin mesh, which corresponds to the case when the concentration in the whole clot region is larger than the critical concentration value,  $c_f$ .

Depending on the choice of parameters, several clot growth patterns can be obtained. In the first case, when the diffusion coefficient is too large and the reaction coefficient is too small, the concentration can be removed by the flow before the clot starts growing and protects the

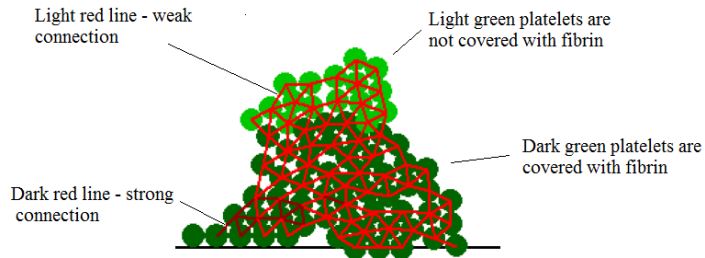


Figure 6: Clot scheme.

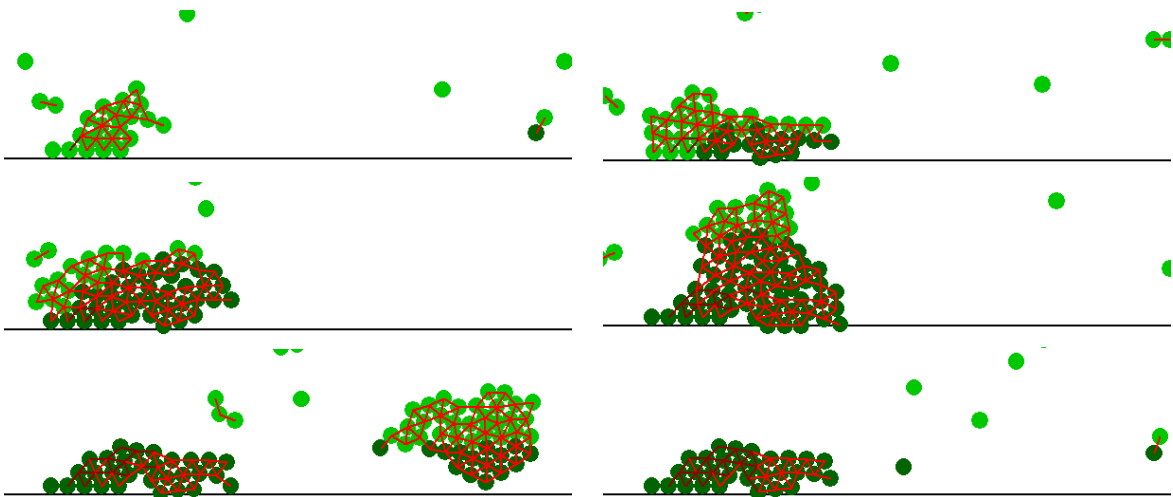


Figure 7: Snapshots of the clot growth for the hybrid model: a) the clot begins to form, b) fibrin begins to cover the growing clot, c) clot core is covered by fibrin but the clot continues to grow, d) the clot reaches its critical size, e) the clot ruptures and its outer part is taken by the flow, f) the core of the clot remains captured in fibrin mesh, which prevents the clot from growing further.

concentration. The second regime is when the concentration production and diffusion rates are such that the concentration slowly covers the clot, but that it is still slower than the clot growth. In that case, when the clot becomes too large to sustain the pressure from the flow, the cap of the clot breaks, leaving the core of the clot covered with fibrin, which stops further clot growth (Figure 9 middle). In the third case, when the rates of concentration production and propagation in the flow are high, the clot grows without rupture until it is completely covered by fibrin (Figure 9 left). The graph on the right side of Figure 9 shows the growth of the clot and the clot core in time. The clot core grows approximately at the same rate as the clot itself.

The second of the three described model behaviours corresponds well to the hypothesis that the clot growth is stopped by the rupture of its covering layer. Figure 7 shows an example in which the clot core is covered by fibrin, and the clot growth is stopped after the rupture of its cap.

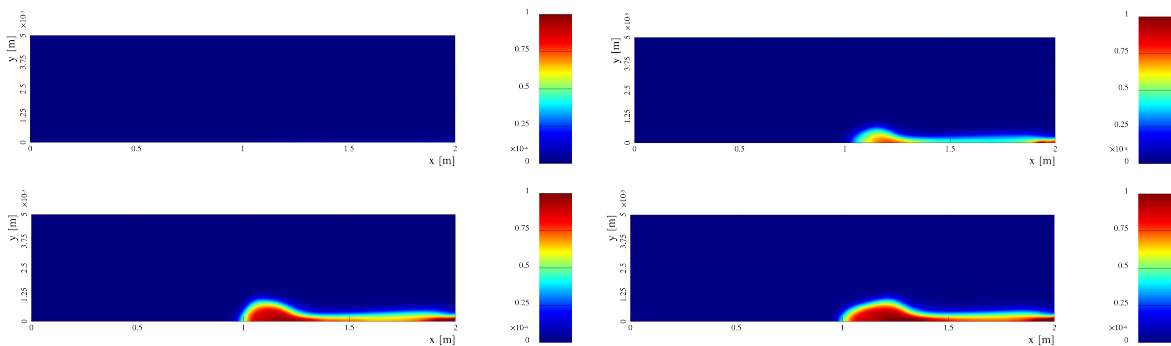


Figure 8: The evolution of the concentration profile in the hybrid model - as the clot grows, it protects the fibrin from being taken away by the flow.

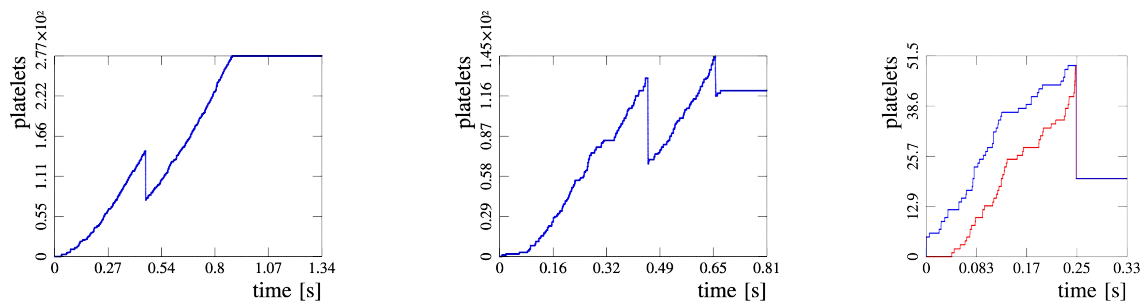


Figure 9: Two cases of clot growth arrest in hybrid model: the fibrin mesh covers the whole clot and stops its growth (left), the clot cap breaks and a part of it is removed by the flow leaving the clot core captured in the fibrin mesh (middle). On the right, an example of the clot growth (blue) is shown together with the clot core (red).

## 4 Discussion

One of the most important problems in the field of hemostasis and thrombosis is related to the question how a thrombus grows and how it stops growing. Various mechanisms have been suggested to act under different conditions, including thrombomodulin-dependent pathway [31], action of flow [32], or fibrin “cap” formation [33]. However, all these mechanisms require fibrin formation, and it is known to be strongly inhibited by the flow [34].

In this work clot growth was studied taking into account the interaction of platelet aggregation with biochemical reactions that participate in blood coagulation. At the first stage of clot growth, platelets aggregate at the injury site. In the beginning, this connection is weak and reversible. After some time it becomes stronger and irreversible due to the participation of other surface receptors which bind platelets to each other. The formation of the platelet aggregate is followed by chemical reactions of blood coagulation in between aggregated platelets. The key point here is that the flow cannot penetrate this clot formed by attached platelets and that, as a consequence, the reactants are not washed out by flow. The biochemical reactions result in the formation of a fibrin network which covers the platelets and does not allow them to attach other platelets from the flow. Finally, when the clot becomes sufficiently large, mechanical stresses from the incoming flow break it removing the weakly attached platelets from its outer part. The core of the clot covered by fibrin network becomes exposed to the flow. It does not attach new platelets, and clot growth stops.

The computational model developed in this work required several consecutive steps. The first step described the plasma flow with platelets without clot growth. In the next step platelet aggregation at the injury site with weak and strong connections was included in order to study the rupture of the clot by the flow. After that a simplified model equation for fibrin concentration was introduced. Though this equation does not describe realistic kinetics of fibrin formation, it allows us to study all the interactions described above. A complete model with more detailed kinetics will be presented in the forthcoming works.

## References

- [1] Davies M.J., *The pathophysiology of acute coronary syndromes*, Heart 2000; 83: 361-366.
- [2] *State-specific mortality from sudden cardiac death*, United States, 1999. MMWR Morb Mortal Wkly Rep 2002; 51: 123-126.
- [3] Ataullakhanov F.I., Panteleev M.A., *Mathematical modeling and computer simulation in blood coagulation* Pathophysiol Haemost Thromb 2005; 34: 60-70.



- [4] Panteleev M.A., Ananyeva N.M., Ataullakhanov F.I., Saenko E.L., *Mathematical models of blood coagulation and platelet adhesion: clinical applications*, Curr Pharm Des 2007; 13: 1457-1467.
- [5] Xu Z., Kamocka M., Alber M., Rosen E.D., *Computational approaches to studying thrombus development*, Arterioscler Thromb Vasc Biol 2011; 31: 500-505.
- [6] Xu Z., Kim O., Kamocka M., Rosen E.D., Alber M., *Multiscale models of thrombogenesis*, Wiley Interdiscip Rev Syst Biol Med 2012; 4: 237-246.
- [7] Orfeo T., Butenas S., Brummel-Ziedins K.E., Gissel M., Mann K.G., *Anticoagulation by factor Xa inhibitors*, J Thromb Haemost 2010; 8: 1745-1753.
- [8] Parunov L.A., Fadeeva O.A., Balandina A.N., Soshitova N.P., Kopylov K.G., Kumskova M.A., Gilbert J.C., Schaub R.G., McGinness K.E., Ataullakhanov F.I., Panteleev M.A., *Improvement of spatial fibrin formation by the anti-TFPI aptamer BAX499: changing clot size by targeting extrinsic pathway initiation*, J Thromb Haemost 2011; 9: 1825-1834.
- [9] Shibeko A.M., Woodle S.A., Lee T.K., Ovanesov M.V., *Unifying the mechanism of recombinant FVIIa action: dose-dependence is regulated differently by tissue factor and phospholipids*, Blood 2012.
- [10] Ohlmann P., Eckly A., Freund M., Cazenave J.P., Offermanns S., Gachet C., *ADP induces partial platelet aggregation without shape change and potentiates collagen-induced aggregation in the absence of Galphaq*, Blood 2000; 96: 2134-2139.
- [11] Panteleev M.A., Balandina A.N., Lipets E.N., Ovanesov M.V., Ataullakhanov F.I., *Task-oriented modular decomposition of biological networks: trigger mechanism in blood coagulation*, Biophys J 2010; 98: 1751-1761.
- [12] Tokarev A.A., Butylin A.A., Ataullakhanov F.I., *Platelet adhesion from shear blood flow is controlled by near-wall rebounding collisions with erythrocytes*, Biophys J 2011; 100: 799-808.
- [13] Shibeko A.M., Lobanova E.S., Panteleev M.A., Ataullakhanov F.I., *Blood flow controls coagulation onset via the positive feedback of factor VII activation by factor Xa*, BMC Syst Biol 2010; 4: 5.
- [14] Jackson S.P., Nesbitt W.S., Westein E., *Dynamics of platelet thrombus formation*, J Thromb Haemost 2009; 7 Suppl 1: 17-20.
- [15] Machlus K.R., Lin F.C., Wolberg A.S., *Procoagulant activity induced by vascular injury determines contribution of elevated factor VIII to thrombosis and thrombus stability in*



- mice*, Blood 2011; 118: 3960-3968.
- [16] Falati S., Gross P., Merrill-Skoloff G., Furie B.C., Furie B., *Real-time in vivo imaging of platelets, tissue factor and fibrin during arterial thrombus formation in the mouse*, Nat Med 2002; 8: 1175-1181.
- [17] Panteleev M.A., Ovanesov M.V., Kireev D.A., Shibeko A.M., Sinauridze E.I., Ananyeva N.M., Butylin A.A., Saenko E.L., Ataulakhanov F.I., *Spatial propagation and localization of blood coagulation are regulated by intrinsic and protein C pathways, respectively*, Biophys J 2006; 90: 1489-1500.
- [18] Kamocka M.M., Mu J., Liu X., Chen N., Zollman A., Sturonas-Brown B., Dunn K., Xu Z., Chen D.Z., Alber M.S., Rosen E.D., *Two-photon intravital imaging of thrombus development*, J Biomed Opt 2010; 15: 016020.
- [19] Kulkarni S., Dopheide S.M., Yap C.L., Ravanat C., Freund M., Mangin P., Heel K.A., Street A., Harper I.S., Lanza F., Jackson S.P., *A revised model of platelet aggregation*, J. Clin. Invest. 2000, V. 105, 6, P. 783-791.
- [20] Fedosov D.A., *Multiscale Modeling of Blood Flow and Soft Matter*, PhD dissertation at Brown University, (2010).
- [21] Groot R.D., Warren P.B., *Dissipative particle dynamics: Bridging the Gap Between Atomistic and Mesoscopic Simulation*, J. Chem. Phys., 107 (1997) (11), 4423–4435.
- [22] Karttunen M., Vattulainen I., Lukkarinen A., *A novel methods in soft matter simulations*, Springer, Berlin, 2004.
- [23] Allen M.P., Tildesley D.J., *Computer Simulation of Liquids*, Clarendon, Oxford, 1987.
- [24] Fedosov D.A., Pivkin I.V., Karniadakis G.E., *Velocity limit in DPD simulations of wall-bounded flows*, J. Comp. Phys. 227 (2008) 25402559.
- [25] Schiller U.D., *Dissipative Particle Dynamics. A Study of the Methodological Background*, Diploma thesis at Faculty of Physics University of Bielefeld, 2005
- [26] Windberger U., Bartholovitsch A., Plasenzotti R., Korak K.J., Heinze G., *Whole blood viscosity, plasma viscosity and erythrocyte aggregation in nine mammalian species: reference values and comparison of data*, Exp. Physiol. 2003, 88:431-440.
- [27] Weisel J.W., *Enigmas of Blood Clot Elasticity*, Science 320, 456 (2008).
- [28] Brown A.E.X., Litvinov R.I., Discher D.E., Purohit P.K., Weisel J.W., *Multiscale Mechanics of Fibrin Polymer: Gel Stretching with Protein Unfolding and Loss of Water*,

Science 325, 741 (2009).

- [29] Tokarev A.A., Butylin A.A., Ermakova E.A., Shnol E.E., Panasenko G.P., and Ataulakhanov F.I., *Finite Platelet Size Could Be Responsible for Platelet Margination Effect*, 2011, Biophys. J. 101 (8): 1835-1843.
- [30] Tokarev A.A., Butylin A.A. and Ataulakhanov. F.I. , *Platelet transport and adhesion in shear blood flow: the role of erythrocytes*, 2012, Computer Research and Modeling, 4 (1): 185200 (article in Russian).
- [31] Panteleev M.A., Ovanesov M.V., Kireev D.A., Shibeko A.M., Sinauridze E.I., Ananyeva N.M., Butylin A.A., Saenko E.L., Ataulakhanov F.I., *Spatial propagation and localization of blood coagulation are regulated by intrinsic and protein C pathways, respectively*, Biophys J., 2006 Mar 1, 90(5), 1489-500.
- [32] Barynin Iu.A., Starkov I.A., Khanin M.A., *Mathematical models in hemostasis physiology*, Izv Akad Nauk Ser Biol. 1999, (1):59-66 (in Russian).
- [33] Kamocka M.M., Mu J., Liu X., Chen N., Zollman A., Sturonas-Brown B., Dunn K., Xu Z., Chen D.Z., Alber M.S., Rosen E.D., *Two-photon intravital imaging of thrombus development*, J. Biomed. Opt. 2010, 15(1):016020.
- [34] Shibeko A.M., Lobanova E.S., Panteleev M.A., Ataulakhanov F.I., *Blood flow controls coagulation onset via the positive feedback of factor VII activation by factor Xa*, BMC Syst. Biol. 2010, 4:5.
- [35] Boryczko K., Yuen D.A., Dzwiniel W., *Finely Dispersed Particles, Micro-, Nano-, and Atto-Engineering*, CRC Press 2005.
- [36] Tosenberger A., Salnikov V., Bessonov N., Babushkina E., Volpert V., *Particle Dynamics Methods of Blood Flow Simulations*, Math. Model. Nat. Phenom. 6 (2011), no. 5, 320–332.
- [37] Pivkin I.V., Karniadakis G.E., *A new method to impose no-slip boundary conditions in dissipative particle dynamics*, J. Comp. Phys. 207 (2005) 114128.

## 5 Appendix. Numerical implementation

In order to develop a simulator for the described model, C++ programming language was used, because it has all the needed features. It is an intermediate-level language which enables rapid and more robust software development and, at the same time, allows a possibility of

“low-level” optimization; it is object-oriented which enables software modularity; it is fast compared to other programming languages with similar abilities; it has a large number of already developed additional libraries, which leaves more time to focus on the writing of model implementation. The integrated development environment (IDE) of choice was MS Visual Studio 2008, accompanied with Microsoft Foundation Classes (MFC) for the development of the graphical user interface, OpenMP for parallelization, and MathGL for the plotting of graphs for the purpose of the analysis of data generated by the simulator. All the code debugging was done in MS Visual Studio.

In DPD simulations most of the total computational time is spent on the calculations of inter-particle forces, therefore this is the part of the code where optimisation would have the largest impact. Usually, the cut-off radius of inter-particle force in DPD ( $r_c$ ) is much smaller than the sizes of the simulation domain, thus calculation of forces between all possible pairs of particles is very inefficient because most of such pairs have an inter-particle distance larger than the cut-off radius. In order to avoid as much of such pairs of particles as possible, the simulation domain, a rectangle in our 2D case, can be divided onto smaller rectangles (called boxes) [35] with lengths of sides equal to  $\min \{x \in \mathbf{R}^+ | x \geq r_c \wedge \exists n \in \mathbf{N} \text{ such that } L = nx\}$  and  $\min \{y \in \mathbf{R}^+ | y \geq r_c \wedge \exists n \in \mathbf{N} \text{ such that } D = ny\}$ , where  $L$  is the length of the domain, and  $D$  is its height. Construction of such rectangular subdivision ensures that for each particle  $p$  we can find its corresponding box  $B_{i,j}$  and that all particles which have non-zero inter-particle force with particle  $p$  are contained in the box  $B_{i,j}$  and 8 surrounding boxes (Figure 10). This eliminates most of the pairs of particles which have a zero inter-particle force, and therefore drastically reduces the computation time. Furthermore, the described domain subdivision enables one to easily parallelize the process of calculation of inter-particle forces by dividing the set of all pairs of “connected” boxes onto multiple disjoint subsets.

Another possibility to decrease simulation time it to increase time step. DPD, due to its definition of conservative force as a finite function, enables a certain increase in the time step compared to other particle methods like Molecular Dynamics. However in our simulation we had to decrease time step more than it was needed just for DPD forces because of the much stronger forces acting between adhered platelets (equation (15)).

## 5.1 Boundary conditions for DPD

As with other particle methods, an important and delicate question is how to define boundary conditions. To simulate a part of blood vessel in our 2D model, three types of boundaries are used - solid, inflow and outflow. Depending on the choice of solid boundary conditions, problems like density oscillations and errors in the velocity profile can occur [24, 36, 37]. Figure 2 shows correct density and velocity profiles for Poiseuille flow obtained with the use of the solid boundary conditions described below.

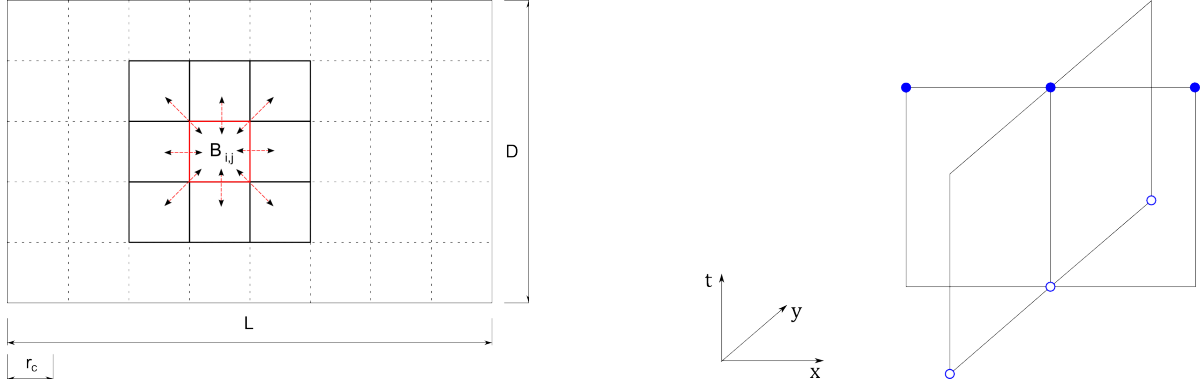


Figure 10: Left: a scheme of the optimization technique for the calculation of inter-particle forces. Right: alternating direction implicit (ADI) method stencil for the first half-step - implicit in the  $x$  and explicit in the  $y$  direction.

The no-slip solid boundary model, which represents the blood vessel wall, is modelled in the following way: if a particle  $p$  is on a distance  $r < r_c$  from the solid boundary, there exists an mirror image  $p'$  of the particle  $p$  on the other side of the boundary with the velocity opposite to velocity of particle  $p$  ( $\mathbf{v}_{p'} \equiv -\mathbf{v}_p$ ). This can seem like adding a fair number of new particles, which can decrease the simulation performance. However, combined with the above described method for the separation of the simulation area on boxes, it can be efficiently implemented without any real addition of new particles. All the mirrored particles are mirror images of particles which are in the boxes connected to the solid boundaries. Therefore, when we calculate forces between two particles in the simulation domain,  $p_1$  and  $p_2$ , if they are positioned in the boxes which are connected to the same solid boundary, we can calculate the force of the imaginary particle  $p'_1$  on the particle  $p_2$  and  $p'_2$  on  $p_1$ . Additionally, if particle  $p$  is on  $r < \frac{1}{2}r_c$  distance from the boundary, the force from  $p'$  on  $p$  is calculated. The described boundary conditions act as no-slip boundary for DPD, and ensure that both, density and velocity, profiles are correct.

The outflow boundary is modelled in the way that all the particles that cross it are being deleted. To ensure a good density distribution near the outflow boundary, an average total force on the particle in the flow is measured and implied in the direction orthogonal to the outflow boundary. In order to know exactly which amount of force to apply on a particle near the outflow boundary, a “total force on a particle” in the direction perpendicular to the outflow boundary is being measured in the bulk of the flow (similar as in [20]). Consider particle  $p_i$  in the bulk of the flow, and suppose that there are  $n$  particles within a  $r_c$  radius of the particle  $p_i$ . Let us denote those particles as  $p_1, \dots, p_n$ , and parts of their coordinates which are orthogonal to the outflow boundary as  $x_1, \dots, x_n$ , and the same with  $x_i$ , the orthogonal part of coordinates of the particle  $p_i$ . Now we can write a total force function for the particle  $p_i$ :

$$F_{p_i}(h) = \frac{1}{2} \sum_{\substack{j=1,\dots,n \\ |x_i-x_j|\geq h}} (\mathbf{F}_{ij}^C + \mathbf{F}_{ij}^D + \mathbf{F}_{ij}^R) \cdot \hat{\mathbf{x}}, \quad (18)$$

where  $\hat{\mathbf{x}}$  is the unit vector orthogonal to the outflow boundary.

To have a more precise force density function, we can take the average of  $F_{p_i}$  for all particles which are not near the outflow boundary. We can also measure the total force over some simulation time and again take the average. With this averaged total force function  $F$ , if some particle is on  $h < r_c$  distance from the outflow boundary, we can apply on it the additional force  $F(h)$  in the direction orthogonal to the boundary. This ensures the correct flux on the outflow boundary.

The inflow boundary is, however, modelled in a more complex way. At the inflow boundary a creation of new particles which will enter our simulation domain is needed. In order to do it correctly and to create plasma and platelet particles with no predefined position, a particle generation area is used in front of our simulation domain (Figure 11). The generation area (GA) works independently of the simulation area (SA). The solid boundaries in GA are modelled in the same way as in SA, but the inflow and outflow boundaries are in fact modelled as periodic boundaries, meaning that the particle that exits GA on the outflow boundary reappears on the GA inflow boundary, creating an infinite flow loop. Also particles from GA do not feel the particles from SA, but the particles from SA feel the particles from GA. For each particle which crosses the GA outflow boundary an exactly same copy is made at the SA inflow boundary, and that new particle is being joined to SA. Once the particle has been joined to SA, it can return for a short time in GA, but it remains assigned to SA and does not influence particles from GA. Furthermore, when it crosses back from GA to SA, it does not generate a new particle. All this insures the integrity and correctness of GA and also the non biased creation of particles for SA.

## 5.2 DPD and PDE data exchange

Since DPD and partial differential equation are solved separately, an exchange period  $\tau$  is introduced as a new parameter. At first the particle system is simulated for a period of time  $\tau$ . During this time the velocity profile is determined, and after it is used to solve the partial differential equation. The PDE is then simulated during the next time interval, the concentration profile is determined and then used in DPD, which finishes one  $\tau$ -cycle of the model. Figure 12 shows one  $\tau$ -cycle.

For each particle the fibrin concentration at the point of its location can be obtained from PDE results of the last  $\tau$ -cycle. One would expect that with the decrease of  $\tau$  a more precise

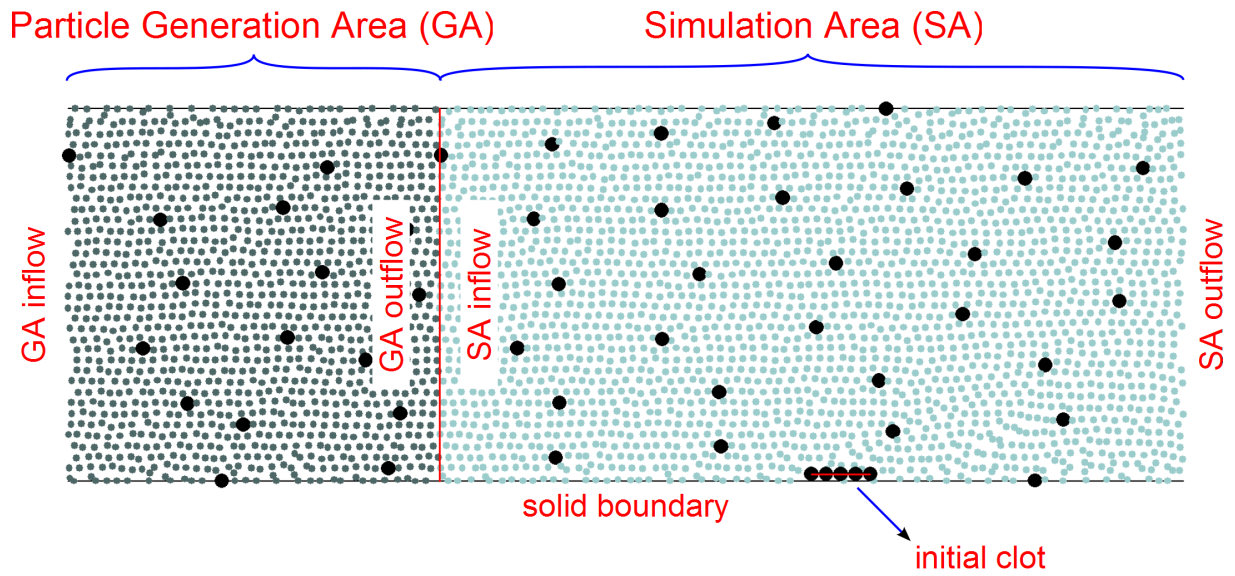


Figure 11: Particle Generation Area (GA) and Simulation Area (SA)

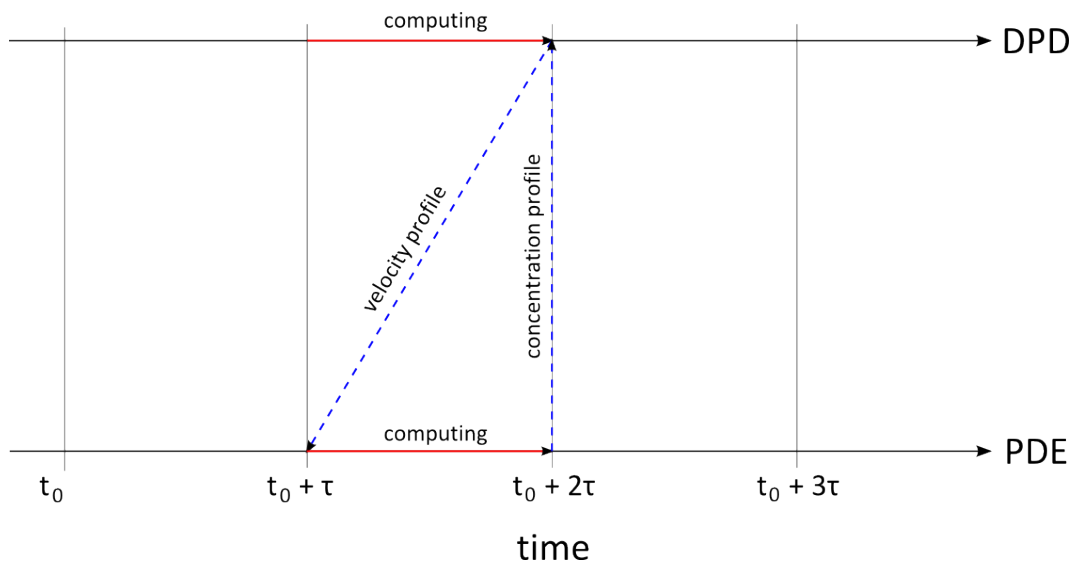


Figure 12: Schematic representation of data exchange between the DPD and PDE submodels.

simulation will be obtained. However, the velocity profile and its local errors influence strongly the evolution of the concentration profile via the convective term in the PDE. In order to obtain a more precise and smoother velocity profile from DPD,  $\tau$  has to be much larger than  $dt$  for DPD, which results in the averaging of particle velocities over a larger number of steps. The ratio of  $\tau : dt$  is highly dependant on the DPD set-up - the number of particles, coefficients of DPD forces, cut-off radius  $r_c$ , the size of mesh used to measure the velocity profile - and is experimentally obtained. The smoothness of velocity profile can be enhanced after the process of measurement with use of smoothing methods. In our work we used a convolution with a Gaussian function.

The PDE is solved on a numerical grid with use of Alternating Direction Implicit (ADI) method. In the described model, Von Neumann boundary conditions were used on the solid spatial boundaries (top and bottom), which represent the blood vessel walls. On the inflow and the outflow boundary, Dirichlet boundary conditions with the zero value were used. The initial concentration values were equal to zero in the whole domain, except at the lower boundary at the place of the initial clot, where the concentration was equal to 1. As the particle method is spatially continuous and thus particles are not restricted to the PDE numerical mesh, a bilinear interpolation is used to calculate the fibrin concentration for the place which a particle occupies.